

GALANTE: finding all the optically accessible Galactic O+B+WR stars in the Galactic Plane

J. Maíz Apellániz¹, E. J. Alfaro^{2,3}, R. H. Barbá⁴, A. Lorenzo²,
A. Marín-Franch^{3,5}, A. Ederoclite^{3,5}, J. Varela^{3,5}, H. Vázquez Ramió^{3,5},
J. Cenarro^{3,5}, D. J. Lennon⁶, and P. García-Lario⁶

¹ Centro de Astrobiología, CSIC-INTA, Madrid, Spain

² Instituto de Astrofísica de Andalucía, CSIC, Granada, Spain

³ Unidad Asociada CEFCA-IAA, CSIC, Teruel, Spain

⁴ Universidad de La Serena, La Serena, Chile

⁵ Centro de Estudios de Física del Cosmos de Aragón, Teruel, Spain

⁶ European Space Agency, ESAC, Madrid, Spain

Abstract

GALANTE is an optical photometric survey with seven intermediate/narrow filters that has been covering the Galactic Plane since 2016 using the Javalambre T80 and Cerro Tololo T80S telescopes. The P.I.s of the northern part (GALANTE NORTE) are Emilio J. Alfaro & Jesús Maíz Apellániz. and the P.I. of the southern part (GALANTE SUR) is Rodolfo H. Barbá. The detector has a continuous 1.4×1.4 field of view with a sampling of $0''.55/\text{pixel}$ and the seven filters are optimized to detect obscured early-type stars. The survey includes long, intermediate, short, and ultrashort exposure times to reach a dynamical range close to 20 magnitudes, something never achieved for such an optical project before. The characteristics of GALANTE allow for a new type of calibration scheme using external Gaia, Tycho-2, and 2MASS data that has already led to a reanalysis of the sensitivity of the Gaia G filter. We describe the project and present some early results. GALANTE will identify the majority of the early-type massive stars within several kpc of the Sun and measure their amount and type of extinction. It will also map the $H\alpha$ nebular emission, identify emission-line stars, and do other studies of low- and intermediate-mass stars.

1 Motivation

GALANTE is a project that is imaging the Galactic Plane (Fig. 1) using the Javalambre T80 and Cerro Tololo T80S twin telescopes [1, 10]. The detector, footprint, exposure times, magnitude range, survey dates, and filters are given in Table 1. The main goal of the project

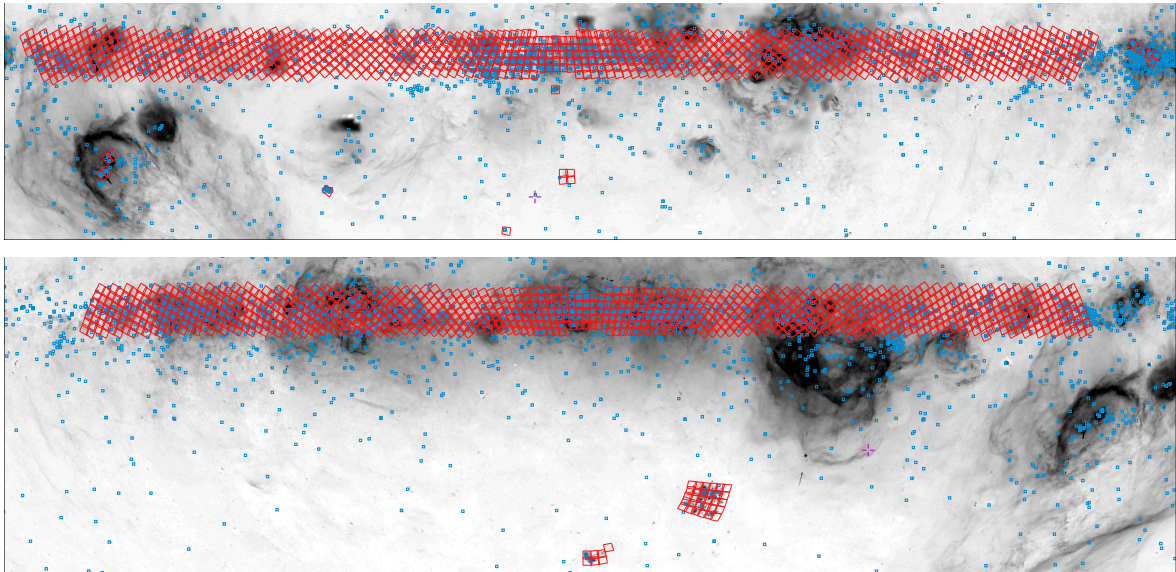


Figure 1: Footprint (red) of the 2009 GALANTE fields divided by hemisphere (top: north, bottom:south). Blue symbols are stars from the Galactic O-Star Catalog (GOSC, [15, 17, 20, 21], <http://gosc.cab.inta-csic.es>), which are mostly O+B+WR stars. The background is an $H\alpha$ image [2] in a log scale aligned with Galactic coordinates using an Aitoff projection. The off-plane fields include the LMC, the SMC (bottom), M31, and M33 (top).

is to identify a near complete sample of Galactic obscured O+B+WR stars up to several kpc and measure their extinction but other objectives will be achieved with the survey. As there are a number of other large-area or whole-sky existing/ongoing photometric surveys (Tycho-2, 2MASS, SDSS, EGAPS, Gaia, Pan-STARRS, J-PLUS, S-PLUS, J-PAS, VVV. . .), the reader may ask him/herself: why one more? Because none has the GALANTE characteristics:

Region of the sky: Some surveys (e.g. SDSS) concentrate in areas away from the Galactic plane, which they do not cover (or do not do it completely). GALANTE covers the Galactic Plane, LMC, SMC, M31, M33, and a few off-plane Galactic clusters.

Magnitude range: Most ground-based surveys use 2-4 m telescopes with one or two exposure times. Hence, they saturate around magnitude 11-12 and cover a dynamic range of 10-12 magnitudes. GALANTE uses 80 cm telescopes with four exposure times to photometer all stars down to magnitude 19-20 (Fig. 2). This is important for obscured stars, which may be close to the detection limit in the blue and be brighter than magnitude 10 beyond 8000 Å.

Filter selection: Some surveys use filter sets not optimized for (e.g. SDSS *ugriz*) or incapable of (e.g. Tycho-2 *BV* or 2MASS *JHK*) measuring the Balmer jump, which is the only realistic method to determine T_{eff} for hot stars [11, 8, 18, 12]. Also, no similar survey includes two narrow filters (on-band and off-band) for $H\alpha$ in order to photometer that line for stars (in absorption or emission) and to map the nebulosity with subarcsecond pixels.

Calibration accuracy: GALANTE uses narrow/intermediate band filters, which are less sensitive to photometric accuracy problems induced by atmospheric extinction.

<i>Detector:</i>	1°4×1°4 continuous FOV with 0'55 pixels.
<i>Footprint:</i>	T80: $ l < 3^\circ + \delta > 0^\circ$ plus selected regions, 1100 sq. dg., Fig. 2. T80S: $ l < 3^\circ + \delta < 0^\circ$ plus selected regions, 1100 sq. dg., Fig. 2.
<i>Exposure times:</i>	2×0.1 s + 2×1 s + 2×10 s + 4×50/100 s (at two different airmasses).
<i>Magnitude range:</i>	Unsat. AB mag 3-17 with S/N > 100 in all filters, detect. to AB mag 19-20.
<i>Survey dates:</i>	GALANTE NORTE (T80): 2016-2021. GALANTE SUR (T80S): 2018-2023.
<i>Filters:</i>	F348M Strömgren <i>u</i> equivalent, T_{eff} + extinction determination. F420N Continuum between H δ and H γ , T_{eff} + extinction determination. F450N Continuum between H γ and H β , T_{eff} + extinction determination. F515N Strömgren <i>y</i> equivalent, T_{eff} + extinction determination. F660N H α line, pure nebular images + emission-line star detection. F665N H α continuum, pure nebular images + emission-line star detection. F861M CaT, tie-in with Gaia-RVS and 2MASS, extinction typing.

Table 1: GALANTE in a nutshell

Confusion: The three-band ($G+G_{\text{BP}}+G_{\text{RP}}$) Gaia photometric survey will address most of the problems above, especially after the full spectrophotometry is available in DR3. However, it will suffer from confusion in crowded and/or nebular regions (common for O+B+WR stars), as the $G_{\text{BP}}+G_{\text{RP}}$ instrument behaves as a slitless spectrograph.

2 Measuring temperature

Figure 3 shows the seven passbands used in the GALANTE survey, four of them in common with the J-PLUS survey [1] (F348M+F515N+F660N+F861M) and three specifically designed for the project (F420N+F450N+F665N). The four bluest filters have been chosen to measure the Balmer jump: F348M measures the continuum to its left while F420N+F450N+F515N do it to the right avoiding the Balmer lines. GALANTE will be used to measure T_{eff} in two steps.

First, we build the two indices (analogous to m_1 and c_1 in the Strömgren system) $m' = \text{F420N} - 1.47 \text{F450N} + 0.47 \text{F515N}$ and $c' = \text{F348M} - 3.44 \text{F420N} + 2.44 \text{F450N}$, where the coefficients were determined empirically. As shown in the left panel of Fig. 4, those indices are nearly independent of gravity, metallicity, and type or amount of extinction for hot stars ($T_{\text{eff}} > 10$ kK) and depend almost only on T_{eff} with a large dynamic range in c' of more than one magnitude between 10 kK and 40 kK. For cooler stars, the position in the index-index diagram depends not only on T_{eff} but also on gravity, and to some extent on the other quantities. The validity of this method is shown on the right panel of Fig. 4, where a preliminary analysis (see below for calibration issues) of one of the GALANTE fields in Cygnus OB2 using aperture photometry correctly places the stellar locus and classifies the stars with known spectral types. Therefore, we will use these indices to give a preliminary estimate of stellar temperature.

As a second step, we will combine GALANTE with 2MASS and process the photometry with CHORIZOS [3], a Bayesian photometric code that allows the simultaneous calculation



Figure 2: GALANTE RGB (F665N+F450N+F420N) image of the Pleiades obtained with the Javalambre T80 telescope. The combination of four exposure times (from 0.1 s to 50 s) yields not a single saturated pixel (despite the presence of the 2nd magnitude Alcyone) while detecting faint objects with magnitudes 19-20. The field of view is 1.4×1.4 with N toward the top and E toward the left.

of T_{eff} , luminosity class, $E(4405 - 5495)$ or amount of extinction, and R_{5495} or type of extinction from photometric data. The output will be combined with Gaia parallaxes to compare trigonometric and spectroscopic distances and build a 3-D extinction map of the solar vicinity more accurate than previous attempts, allowing for different types of extinction.

3 Photometric calibration

The primary photometric calibration of GALANTE uses the fact that a typical 1.4×1.4 Galactic Plane field contains ~ 100 objects with good-quality Tycho-2 $B_T + V_T$ + Gaia $G + G_{\text{BP}} + G_{\text{RP}}$ + 2MASS $J + H + K$ (8 filters) and $\sim 10^4$ objects with their Gaia and 2MASS equivalents (6 filters). We process that input photometry with CHORIZOS [3] and the SED grid of [7] to generate synthetic predicted magnitudes (and their uncertainties) in each of the seven GALANTE filters allowing for arbitrary variations in T_{eff} , luminosity class, $E(4405 - 5495)$, and R_{5495} . The resulting predicted uncertainties for a single star are in the range of one hundredth to a few tenths of magnitude, with lower values for objects with 8-filter photometry and lower input uncertainties and for redder filters. For each field and filter we first combine the information from the $\sim 10^4$ objects with 6-filter photometry to detect (and correct if necessary) possible low-order flat-field issues and we then use objects with 8-filter photometry to calculate the zero point, which has a typical uncertainty of one hundredth of a magnitude. The whole process is dependent on the accuracy of the calibration

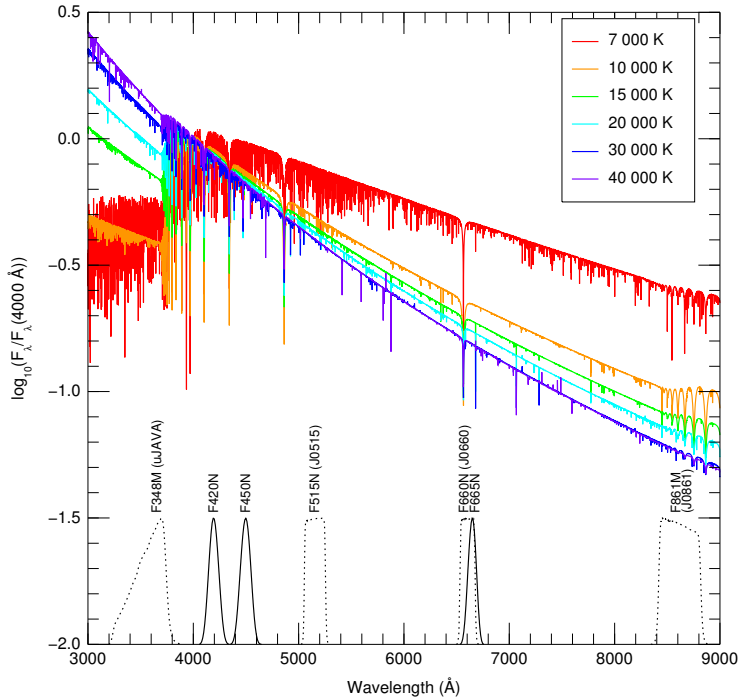


Figure 3: Normalized passbands for the seven GALANTE filters compared with model SEDs of stars with different T_{eff} [7]. The filter combination F438M+F420N+F450N+F515N has been chosen to accurately measure the Balmer jump using continuum regions that avoid the strong Balmer lines. J-PLUS filters are plotted with dotted lines and filters exclusive to GALANTE are plotted with solid lines.

of the input photometry (Tycho-2, Gaia, and 2MASS), to which we have devoted a strong effort until being satisfied [4, 5, 6, 9, 13, 14]. The right panel of Fig. 4 shows how well this works even with a preliminary version in which we used (a) aperture instead of PSF photometry and (b) the ~ 100 object calibration sample and only six filters (it was done before Gaia DR2 so no $G_{\text{BP}}+G_{\text{RP}}$ photometry was available and we used the calibrations of [6] and [9] instead of those of [13] and [14]).

We also use several secondary calibration mechanisms:

- Comparison of results for the same field using different exposure times and air masses to check for anomalous detector effects or atmospheric extinction.
- Comparison between adjacent fields. The GALANTE strategy leaves a generous overlap ($\sim 12'$) between fields to allow for the identification of possible zero point offsets.
- Use of spectrophotometric standards. Note that the GALANTE FOV is large enough that $\sim 10\%$ of the fields have standards of one type or another. Also note that we have recently increased the sample of spectrophotometric standards [14].
- Use as CHORIZOS input the temperature and gravity of objects with accurate spectroscopic classifications, especially early-type stars for which the intrinsic SED is well known. This leads to reduced uncertainties for the predicted magnitudes. For this purpose we use the spectral classifications from the Galactic O-Star Spectroscopic Survey (GOSSS, [16, 19, 22, 23]).

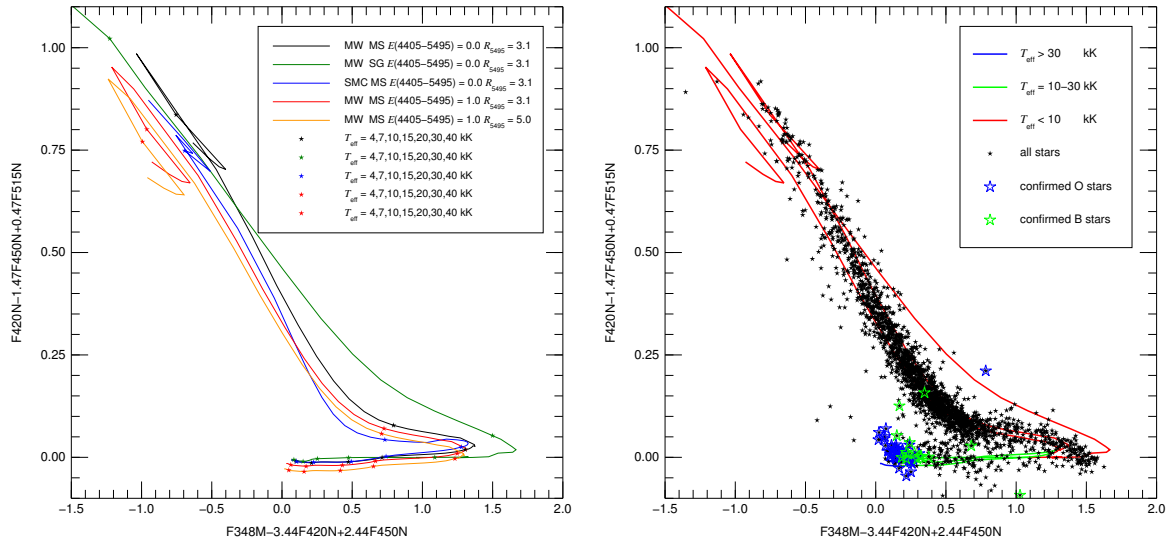


Figure 4: [left] A index-index diagram using model SEDs from [7]. Note how we can measure T_{eff} for hot stars (lower branch) independently of gravity, metallicity, and reddening. [right] Same diagram with only the first, second, and fourth synthetic photometry functions plus overplotted data from one of the GALANTE fields in Cygnus OB2 (using a preliminary calibration). Most of the stars in the diagram follow the main-sequence track between A and K stars, as expected. The field contains a very rich highly extinguished OB association. This results in few late-B stars present (they are too dim for GALANTE at the distance and extinction of the association) but also in 100+ O and early B stars detected. Despite their high extinction ($A_V \sim 6$ mag), they are at the expected location in the diagram and the existing spectral types confirm their nature, thus providing an indication of the excellent quality of the data and calibration.

4 Objectives and planning

The main objective of GALANTE is to identify all Galactic O+B+WR stars down to magnitude 17 and estimate their T_{eff} . We will cross-match all OBA stars with 2MASS and measure their $E(4405 - 5495)$ and R_{5495} . We will coordinate our efforts with the Stellar, Circumstellar, and Interstellar Physics WEAVE survey and with GOSSS to acquire follow-up spectroscopy of the newly found O+B+WR stars.

Some additional objectives include (a) a magnitude-limited catalog of emission-line stars, (b) the IMF of large-area clusters and associations, (c) a continuum-subtracted $H\alpha$ map with subarcsecond pixels, and (d) cross-calibration with Gaia.

GALANTE NORTE started taking data in 2016 and GALANTE SUR in 2018. If weather behaves, we should complete the northern survey in 2021 and the southern one in 2023. For the long-term future several extensions are possible: deep surveys of interesting regions, multiple epochs, and additional filters are some of the possibilities.

Acknowledgments

Based on observations made with the JAST/T80 telescope at the Observatorio Astrofísico de Javalambre, in Teruel, owned, managed and operated by the Centro de Estudios de Física del Cosmos de Aragón. J.M.A., E.J.A., and A.L. acknowledge support from the Spanish Government Ministerio de Ciencia, Innovación y Universidades through grant AYA2016-75 931-C2-1/2-P. R.H.B. acknowledges support from DIDULS project PR18143.

References

- [1] Cenarro, A. J. et al. 2017, HSA IX, 11
- [2] Finkbeiner, D. P. 2003, ApJS 146, 407
- [3] Maíz Apellániz, J. 2004, PASP 116, 859
- [4] Maíz Apellániz, J. 2005, PASP 117, 615
- [5] Maíz Apellániz, J. 2006, AJ 131, 1184
- [6] Maíz Apellániz, J. 2007, ASPC 364, 227
- [7] Maíz Apellániz, J. 2013a, HSA VII, 657
- [8] Maíz Apellániz, J. 2013b, HSA VII, 583
- [9] Maíz Apellániz, J. 2017, A&A 608, L8
- [10] Maíz Apellániz, J. 2017, Early Data Release + Scientific Exploitation of the J-PLUS Survey, 15
- [11] Maíz Apellániz, J. & Sota, A. 2018, RMxAC 33, 44
- [12] Maíz Apellániz, J. & Barbá, R. H. 2018, A&A 613, A9
- [13] Maíz Apellániz, J. & Pantaleoni González, M. 2018, A&A 616, L7
- [14] Maíz Apellániz, J. & Weiler, M. 2018, arXiv:1808.02820, A&A accepted
- [15] Maíz Apellániz, J. et al. 2004, ApJS 151, 103
- [16] Maíz Apellániz, J. et al. 2011, HSA VI, 467
- [17] Maíz Apellániz, J. et al. 2012, ASPC 465, 484
- [18] Maíz Apellániz, J. et al. 2014, A&A 564, A63
- [19] Maíz Apellániz, J. et al. 2016, ApJS 224, 4
- [20] Maíz Apellániz, J. et al. 2017b, HSA IX, 509
- [21] Sota, A. et al. 2008, RMxAC 33, 56
- [22] Sota, A. et al. 2011, ApJS 193, 24
- [23] Sota, A. et al. 2014, ApJS 211, 10